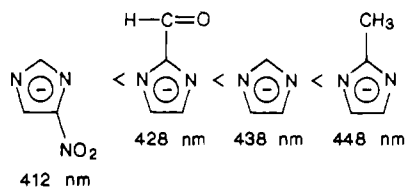


the  $\pi$ -acceptor power of the ring. However, the pyridine N-heterocycles are legitimately aromatic in character, while the imidazole rings are quasi-aromatic. The results here show that a sufficiently conjugated chromophore induces the same MLCT behavior and increase in the  $\pi$ -acceptor capacity as related chromophores in the pyridine N-heterocycles. The band positions for the cases  $R = \text{CO}_2^-$ ,  $\text{CHO}$ , and  $\text{NO}_2$  are in the proper order with respect to their  $\sigma_p$  constants ( $\leq 0.13, 0.22, 0.78$ ).<sup>7</sup> Electrochemistry of the  $(\text{NH}_3)_5\text{Ru}(\text{2CHOimH})^{2+}$  complex supports  $\text{2CHOimH}$  as intermediate between pyridine and pyrazine as a  $\pi$  acceptor.<sup>12</sup>

The imidazolato forms of all of the RimH ligands are superior as  $\pi$  donors due to the additional anionic charge density within the five-membered ring. This is borne out by the LMCT  $\pi_{2,n}$  band positions of the  $(\text{CN})_5\text{Fe}^{\text{III}}(\text{R-imidazolato})$  series:



The order is inverted as the best  $\pi$ -donor occurs with the best releasing R group, which is  $R = \text{CH}_3$  in this series. Although the very rapid dissociation of  $(\text{CN})_5\text{Fe}(\text{2CO}_2\text{im})^{4-}$  has prevented the observation of its  $\pi_{2,n}$  LMCT band in this study, one would anticipate a value intermediate between those for  $R = \text{CHO}$  and  $R = \text{H}$ . Therefore, if the  $(\text{CN})_5\text{Fe}(\text{2CO}_2\text{im})^{4-}$  complex were observed in a rapid flow study, for example, the estimated position of the band maximum should be  $\sim 433$  nm.

The steric influence plus the anionic charge of  $\text{2CO}_2\text{imH}^-$  significantly reduces the affinity of this imidazole toward  $(\text{CN})_5\text{Fe}^{2+}$  by about  $5 \times 10^3$  in equilibrium constant.<sup>1,19</sup> This does not appear to be caused by a reduction in the  $\sigma$  donation of the pyridine nitrogen of this ring because the  $\text{p}K_a \approx 7.2$  is close to the parent imidazole  $\text{p}K_a$  of 7.0; we note here that the  $\sigma$ -withdrawal influence of  $R = \text{CO}_2^-$  is compensated by an additional electrostatic attraction for cationic species including  $\text{H}^+$ ,  $\text{Ru}(\text{NH}_3)_5^{2+}$ ,

and  $\text{Ru}(\text{NH}_3)_5^{3+,12}$ . The cations are not anomalously low in their affinities for  $\text{2CO}_2\text{imH}^-$ . In fact the more withdrawing group  $R = \text{CHO}$  produces stable complexes for both  $\text{Fe}(\text{II})$  and  $\text{Fe}(\text{III})$  in the  $(\text{CN})_5\text{FeL}^{n-}$  series. Therefore, a neutral ligand that will be a slightly poorer  $\sigma$  base than  $\text{2CO}_2\text{imH}^-$  still produces a more stable net interaction with  $(\text{CN})_5\text{Fe}^{2+}$ ; the influence is clearly even more important for the  $\text{Fe}(\text{II})$  system, where  $(\text{CN})_5\text{Fe}^{3+}$  shows no measurable affinity at all for  $\text{2CO}_2\text{imH}^-$  (cf. <sup>13</sup>C NMR results, Figure 7).

A number of observations relevant to the ligand substitution processes involving the  $(\text{CN})_5^{2-}$  moiety have been observed. The dissociation of the 2-methylimidazolato ligand is reasonably representative and worthy of some detailed consideration.

The current assessment of the dissociation of 2-methylimidazolato ligand from  $(\text{CN})_5^{2-}$  is as follows:

(1) The approach to equilibrium rate constant does not have a significant term due to the back-reaction ( $k_{\text{obsd}}$  appears to be independent of  $[\text{L}]$ ), in contrast to the imidazolato case where  $k_{\text{obsd}}$  increases linearly with  $[\text{L}]$ . This is readily interpreted as a steric inhibition to the rate of substitution of 2-methylimidazole that is absent for the unhindered imidazole.

(2) The presence of the  $\text{CH}_3$  group accelerates the  $k_0$  path about 8.9 times at 25.0 °C relative to that for  $R = \text{H}$ , consistent with a steric effect of ca. 1.3 kcal/mol as observed previously.<sup>1,19</sup> Strained coordination is substantially more prone to redox catalysis for ligand displacement, which causes complications in the study of the  $\text{2CH}_3\text{imH}$  complex.

(3) An oxidation product of  $\text{2CH}_3\text{imH}$ ,  $\text{2CO}_2\text{imH}^-$ , undergoes a similar, but very rapid, ligand dissociation reaction for the imidazolato form of the complex,  $(\text{CN})_5\text{Fe}(\text{2CO}_2\text{im})^{4-}$ .

**Acknowledgment.** We gratefully acknowledge support from NSF Grants CHE 802183 and CHE 8417751.

**Registry No.**  $(\text{CN})_5\text{Fe}^{\text{III}}(\text{2CH}_3\text{imH})^{2-}$ , 74354-02-2;  $(\text{CN})_5\text{Fe}^{\text{III}}(\text{2CO}_2\text{imH})^{3-}$ , 109432-48-6;  $(\text{CN})_5\text{Fe}^{\text{III}}(\text{2CHOimH})^{2-}$ , 109432-49-7;  $(\text{CN})_5\text{Fe}^{\text{II}}(\text{2CH}_3\text{imH})^{3+}$ , 60105-86-4;  $(\text{CN})_5\text{Fe}^{\text{II}}(\text{2CO}_2\text{imH})^{4-}$ , 109432-50-0;  $(\text{CN})_5\text{Fe}^{\text{II}}(\text{2CHOimH})^{3-}$ , 109432-51-1;  $\text{S}_2\text{O}_8^{2-}$ , 15092-81-6.

**Supplementary Material Available:** UV-visible spectra (Figures 1SM-5SM) (5 pages). Ordering information is given on any current masthead page.

## Notes

Contribution from the Institute for Physical and Theoretical Chemistry, University of Frankfurt, 6000 Frankfurt am Main, FRG, and Institute for Inorganic Chemistry, University of Witten/Herdecke, 5810 Witten-Annen, FRG

### High-Pressure Kinetic Study of an Unusual Hydrolysis Reaction of (Hexafluoroacetylacetonato)bis(ethylenediamine)cobalt(III) in Aqueous Solution

Y. Kitamura<sup>1</sup> and R. van Eldik\*

Received February 5, 1987

In general, high-pressure kinetic studies and the associated construction of reaction volume profiles can assist the assignment of the intimate nature of the mechanism for a wide range of thermal and photochemical reactions in solution.<sup>2-4</sup> These include substitution, isomerization, addition/elimination, and electron-transfer processes.

\* To whom correspondence should be addressed at the University of Witten/Herdecke.

Our interest in recent years in the mechanism of base hydrolysis reactions of  $\text{Co}(\text{III})$  complexes<sup>5,6</sup> has led to a series of detailed studies of an unusual, reversible hydrolysis reaction of  $\text{Co}(\text{en})_2(\text{hfac})^{2+}$  ( $\text{en} = \text{ethylenediamine}$ ,  $\text{hfac} = \text{hexafluoroacetylacetonato}$ ) in aqueous solution.<sup>7,8</sup> During this reaction, addition of  $\text{OH}^-$  to the carbonyl carbon atom of the  $\text{hfac}$  ligand occurs, as indicated in reaction 1. The structure of the hydrolysis product was recently confirmed by a crystal structure determination.<sup>9</sup> A kinetic study<sup>6</sup>

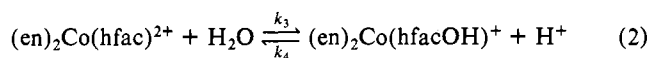
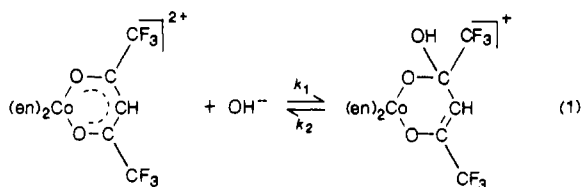
- (1) On leave from the Department of Chemistry, Ehime University, Matsuyama 790, Japan, as a research fellow of the Department of Education of Japan.
- (2) van Eldik, R. *Angew. Chem., Int. Ed. Engl.* **1986**, *25*, 673.
- (3) van Eldik, R. *Comments Inorg. Chem.* **1986**, *5*, 135.
- (4) van Eldik R., Ed. *Inorganic High Pressure Chemistry: Kinetics and Mechanisms*; Elsevier: Amsterdam, 1986.
- (5) Kitamura, Y.; van Eldik, R.; Kelm, H. *Inorg. Chem.* **1984**, *23*, 2038.
- (6) van Eldik, R.; Kitamura, Y.; Piriz Mac-Coll, C. R. *Inorg. Chem.* **1986**, *25*, 4252.
- (7) Aygen, S.; Kitamura, Y.; Kuroda, K.; Kume, R.; Kelm, H.; van Eldik, R. *Inorg. Chem.* **1985**, *24*, 423.
- (8) Kitamura, Y.; van Eldik, R. *Transition Met. Chem.* **1984**, *9*, 257.
- (9) Aygen, S.; Paulus, E. F.; Kitamura, Y.; van Eldik, R. *Inorg. Chem.* **1987**, *26*, 769.

**Table I.** Pressure Dependence of  $k_{\text{obsd}}$  as a Function of pH<sup>a</sup>

pH <sup>c</sup>	$k_{\text{obsd}},^b \text{ s}^{-1}$				
	$P = 2 \text{ MPa}$	$P = 50 \text{ MPa}$	$P = 100 \text{ MPa}$	$P = 150 \text{ MPa}$	$P = 190 \text{ MPa}$
5.92	193	148	106	76	86
6.11	111	132	87	82	57
6.28	66.9	57.5	56.0	48.6	50.0
6.41	50.5	50.6	47.1	41.5	40.3
6.65	36.0	30.2	28.3	23.2	20.5
6.86	30.3	26.6	25.2	25.2	25.0
$10^{-8} dk_{\text{obsd}}/da_{\text{H}},^d \text{ M}^{-1} \text{ s}^{-1}$	$1.55 \pm 0.12$	$1.38 \pm 0.20$	$0.94 \pm 0.08$	$0.71 \pm 0.17$	$0.78 \pm 0.07$
9.08	20.6	27.0	33.6	43.3	54.1
9.18	24.6	30.0	37.6	44.8	63.6
9.24	26.1	34.4	44.8	70.3	
9.50	45.2	56.1	84.8	93.4	
$10^{-6} dk_{\text{obsd}}/da_{\text{OH}},^d \text{ M}^{-1} \text{ s}^{-1}$	$1.27 \pm 0.05$	$0.92 \pm 0.04$	$1.03 \pm 0.06$	$0.64 \pm 0.17$	0.55

<sup>a</sup> [Co(III)] = 25 mM,  $T = 25 \text{ }^\circ\text{C}$ , ionic strength = 1.07 M, wavelength = 550 (pH < 7) and 470 nm (pH > 9). <sup>b</sup> Mean value of four runs with an average standard deviation of 5%. <sup>c</sup> pH value at ambient pressure. <sup>d</sup> Calculated by using the corrected pH values in Table II (see text).

of the hydrolysis process at ambient pressure led to the suggested mechanism in (1) and (2), for which the empirical rate law is given in (3). Analysis of the data resulted in the following values at



$$k_{\text{obsd}} = k_a + k_b[\text{H}^+] + k_c[\text{OH}^-] \quad (3)$$

25 °C and 1 M ionic strength (Tris buffer):  $k_a (=k_2 + k_3) = 5.9 \text{ s}^{-1}$ ;  $k_b (=k_4) = 9.9 \times 10^7 \text{ M}^{-1} \text{ s}^{-1}$ ;  $k_c (=k_1) = 2.9 \times 10^6 \text{ M}^{-1} \text{ s}^{-1}$ . The last two rate constants can be determined accurately via  $T$ -jump measurements at pH < 7 and pH > 9, respectively.

We have now studied the pressure dependencies of  $k_1$  and  $k_4$ , which along with the overall reaction volume<sup>10</sup> enable us to construct volume profiles for both processes. The results are discussed in reference to activation volume data for related addition and elimination reactions and volume profiles for base-catalyzed substitution reactions.

### Experimental Section

[Co(en)<sub>2</sub>hfac](ClO<sub>4</sub>)<sub>2</sub> was prepared and characterized as described previously.<sup>7</sup> Chemicals of analytical grade and doubly distilled water were used throughout this study. The pH of the test solutions was measured at ambient pressure by using a Radiometer pHM 64 instrument equipped with a reference electrode filled with a saturated NaCl solution to prevent the precipitation of KClO<sub>4</sub>. Kinetic measurements at elevated pressures were performed on a Joule-heating  $T$ -jump instrument<sup>11</sup> thermostated at  $22.0 \pm 0.1 \text{ }^\circ\text{C}$ . Under the selected experimental conditions, a discharge of 25 kV results in a temperature-jump of ca. 3 °C at an ionic strength of 1 M,<sup>8</sup> so that the relaxation temperature is in fact 25 °C. Buffer solutions were prepared by adding appropriate quantities of 1 M HClO<sub>4</sub> or 1 M NaOH to 2 cm<sup>3</sup> of a 2 M Tris–2M MES<sup>12</sup> solution and diluting to 10 cm<sup>3</sup>, during which NaClO<sub>4</sub> was added to adjust the ionic strength to 1 M. Reaction volumes were determined with the aid of a Carlsberg dilatometer as described previously,<sup>13</sup> for which the temperature was controlled at  $25.0 \pm 0.002 \text{ }^\circ\text{C}$ .

### Results and Discussion

Kinetic measurements were performed in two acidity ranges as a function of pH and pressure. These conditions were selected on the basis of our earlier work at ambient pressure,<sup>8</sup> and the first-order rate constants were determined in a similar way using

**Table II.** Estimated Pressure Dependence of pH and pOH

$P, \text{ MPa}$	$(\text{pH})_P - (\text{pH})_{0.1}$	$(\text{pOH})_P - (\text{pOH})_{0.1}$	$P, \text{ MPa}$	$(\text{pH})_P - (\text{pH})_{0.1}$	$(\text{pOH})_P - (\text{pOH})_{0.1}$
50	0.034	-0.219	150	0.095	-0.604
100	0.066	-0.420	190	0.116	-0.742

the high-pressure modification.<sup>11</sup> The observed rate constants at the lowest pressure (2 MPa) are in close agreement with those reported at ambient pressure (0.1 MPa)<sup>8</sup> (see Table I). Throughout the series of data,  $k_{\text{obsd}}$  increases with increasing [H<sup>+</sup>] in the low-pH region and increases with increasing [OH<sup>-</sup>] in the high pH region. The slopes of  $k_{\text{obsd}}$  vs. [H<sup>+</sup>], i.e.  $k_4$ , and [OH<sup>-</sup>], i.e.  $k_1$ , decrease with increasing pressure, indicating that the volume of activation is positive in both cases. However, in order to determine its exact value, one must consider the pressure dependencies of the acid dissociation constants of the buffer employed, the ion product of water, and the activity coefficients of the ionic species. This is done in the following sections.

For the buffer system used in this study, the pH of a particular solution can be expressed as in eq 4,<sup>14</sup> where [T], [TH<sup>+</sup>], [M],

$\text{pH} = 0.5(\text{p}K_{\text{M}} + \text{p}K_{\text{T}}) + 0.5 \log\{[\text{T}][\text{M-H}^-]/[\text{M}][\text{TH}^+]\}$  (4)

and [M-H<sup>-</sup>] represent the molar concentrations of Tris, protonated Tris, MES, and deprotonated MES, respectively.  $K_{\text{M}}$  and  $K_{\text{T}}$  are the acid dissociation constants of MES and TrisH<sup>+</sup>, respectively. Since [T], [TH<sup>+</sup>], [M], and [M-H<sup>-</sup>] can be assumed to be independent of pressure,<sup>15</sup> the pressure dependence of pH and pOH can be expressed as in (5) (with  $P$  in units of MPa),<sup>14</sup> and the

$$\begin{aligned}
 (\text{pH})_P - (\text{pH})_{0.1} &= 7.18 \times 10^{-4}P / (1 + 9.2 \times 10^{-4}P) \\
 (\text{pOH})_P - (\text{pOH})_{0.1} &= -45.8 \times 10^{-4}P / (1 + 9.2 \times 10^{-4}P) \quad (5)
 \end{aligned}$$

corresponding values are summarized in Table II. These corrected  $(\text{pH})_P$  and  $(\text{pOH})_P$  values were used to estimate  $dk_{\text{obsd}}/da_{\text{OH}}$  and  $dk_{\text{obsd}}/da_{\text{H}}$  from the data in Table I.

In the basic region (pH 9), rate law 3, reduces to (6). Since we are dealing with an ionic process,  $k_1$  is expected to depend on

$$k_{\text{obsd}} = k_a + k_1[\text{OH}^-] = k_a + k_1 a_{\text{OH}} / \gamma_{\text{OH}} \quad (6)$$

the ionic composition of the medium according to eq 7, where  $\gamma_c$

$$k_1 = k_1^\circ \gamma_c \gamma_{\text{OH}} / \gamma_\ddagger \quad (7)$$

and  $\gamma_\ddagger$  are the activity coefficients of the complex and transition

(10) Kitamura, Y. *Bull. Chem. Soc. Jpn.* **1985**, *58*, 2699.

(11) Doss, R.; van Eldik, R.; Kelm, H. *Rev. Sci. Instrum.* **1982**, *53*, 1592.

(12) Tris = tris(hydroxymethyl)aminomethane; MES = 2-morpholinoethanesulfonic acid.

(13) Kitamura, Y.; van Eldik, R. *Ber. Bunsen-Ges. Phys. Chem.* **1984**, *88*, 418.

(14) Kitamura, Y.; Itoh, T. *J. Solution Chem.*, in press.

(15) The following relationships hold at each pressure:  $[\text{TH}^+][\text{M-H}^-]/[\text{T}][\text{M}] = K_{\text{M}}/K_{\text{T}}\gamma_+\gamma_-$ ;  $[\text{T}] + [\text{TH}^+] = 0.4 \text{ M}$ ;  $[\text{M}] + [\text{M-H}^-] = 0.4 \text{ M}$ ;  $[\text{TH}^+] = [\text{M-H}^-] + [\text{HClO}_4]$ . In these expressions [HClO<sub>4</sub>] represents the added concentration of HClO<sub>4</sub>, and  $\gamma_+$  and  $\gamma_-$  represent the activity coefficients of TH<sup>+</sup> and M-H<sup>-</sup>, respectively. The pressure dependencies of  $K_{\text{M}}$  and  $K_{\text{T}}$  are quite similar,<sup>14</sup> viz.  $-RT \text{ d} \ln K_{\text{M}}/\text{d}P = 3.9$  and  $-RT \text{ d} \ln K_{\text{T}}/\text{d}P = 4.3 \text{ cm}^3 \text{ mol}^{-1}$ , such that when one neglects the rather trivial pressure dependence of  $\gamma_+\gamma_-$ , the above relationships are all independent of pressure.

**Table III.**  $\Delta V^\ddagger$  and  $\Delta \bar{V}$  Data for Reactions 1 and 2 as a Function of Ionic Strength at 25 °C<sup>a</sup>

vol param	$\mu = 0$	$\mu = 1.1 \text{ M}$
$\Delta V^\ddagger(k_1)$	$+14.5 \pm 2.3$	$+9.2 \pm 2.3$
$\Delta V^\ddagger(k_2)$	$+3.8 \pm 2.4$	$+2.9 \pm 2.3$
$\Delta \bar{V}(\text{reacn 1})$	$+10.7 \pm 0.1$	$+6.3 \pm 0.0$
$\Delta V^\ddagger(k_3)$	$-4.7 \pm 2.2$	$-4.2 \pm 2.1$
$\Delta V^\ddagger(k_4)$	$+6.7 \pm 2.1$	$+9.4 \pm 2.1$
$\Delta \bar{V}(\text{reacn 2})$	$-11.4 \pm 0.1$	$-13.6 \pm 0.0$

<sup>a</sup> All volume quantities quoted in  $\text{cm}^3 \text{mol}^{-1}$ .

states, respectively, and  $k_1^\circ$  is the rate constant at infinite dilution. It follows that the volume of activation for  $k_1$  can be given as expressed in (8). Furthermore, differentiation of (6) with respect

$$\Delta V^\ddagger(k_1) = \Delta V^\ddagger(k_1^\circ) - RT \frac{d}{dP} \ln (\gamma_c \gamma_{\text{OH}} / \gamma_*) \quad (8)$$

to  $a_{\text{OH}}$  results in (9), which along with the expression in (8) results in (10). It was recently pointed out by Hamann that the pressure

$$dk_{\text{obsd}}/da_{\text{OH}} = k_1/\gamma_{\text{OH}} \quad (9)$$

$$\Delta V^\ddagger(k_1) = -RT \frac{d}{dP} \left( \ln \frac{dk_{\text{obsd}}}{da_{\text{OH}}} \right) - RT \frac{d \ln \gamma_{\text{OH}}}{dP}$$

$$\Delta V^\ddagger(k_1^\circ) = -RT \frac{d}{dP} \left( \ln \frac{dk_{\text{obsd}}}{da_{\text{OH}}} \right) + RT \frac{d}{dP} \left( \ln \frac{\gamma_c}{\gamma_*} \right) \quad (10)$$

dependence of an activity coefficient can be predicted by the limiting Debye-Hückel relationship even at high ionic strength.<sup>16</sup> It follows that the pressure dependence of the activity coefficient of an ion with charge  $Z_i$  is given by eq 11, where  $\rho$  and  $\epsilon$  are the

$$\frac{d \ln \gamma_i}{dP} = -809 Z_i^2 \mu^{1/2} \frac{d}{dP} (\rho/\epsilon^3)^{1/2} \quad (11)$$

density and dielectric constant of water, respectively, and  $d(\rho/\epsilon^3)^{1/2}/dP = -6.6 \times 10^{-7} \text{ MPa}^{-1}$  at 25 °C.<sup>17</sup> With  $Z_c = 2$  and  $Z_* = 1$  eq 10 can now be modified to (12).

$$\Delta V^\ddagger(k_1) = -RT \frac{d}{dP} \left( \ln \frac{dk_{\text{obsd}}}{da_{\text{OH}}} \right) - 1.3 \text{ cm}^3 \text{ mol}^{-1}$$

$$\Delta V^\ddagger(k_1^\circ) = -RT \frac{d}{dP} \left( \ln \frac{dk_{\text{obsd}}}{da_{\text{OH}}} \right) + 4.0 \text{ cm}^3 \text{ mol}^{-1} \quad (12)$$

The kinetic data in the acidic region ( $\text{pH} < 7$ ) can be treated in a similar way, for which the rate law (3) reduces to (13) and the corresponding expressions for the volumes of activation are given in (14). The values of  $dk_{\text{obsd}}/da_{\text{OH}}$  and  $dk_{\text{obsd}}/da_{\text{H}}$  in Table

$$k_{\text{obsd}} = k_a + k_4[\text{H}^+] = k_a + k_4 a_{\text{H}}/\gamma_{\text{H}} \quad (13)$$

$$\Delta V^\ddagger(k_4) = -RT \frac{d}{dP} \left( \ln \frac{dk_{\text{obsd}}}{da_{\text{H}}} \right) - 1.3 \text{ cm}^3 \text{ mol}^{-1}$$

$$\Delta V^\ddagger(k_4^\circ) = -RT \frac{d}{dP} \left( \ln \frac{dk_{\text{obsd}}}{da_{\text{H}}} \right) - 4.0 \text{ cm}^3 \text{ mol}^{-1} \quad (14)$$

I were used to calculate the volumes of activation for  $k_1$  and  $k_4$  with the aid of eq 12 and 14, respectively, and the results are summarized in Table III. Before we turn to a discussion of these data, it is important to indicate how the volumes of activation for the reverse reactions ( $k_2$  and  $k_3$ ) were obtained. The reaction volume for reaction 1 was measured dilatometrically at 1 M ionic strength (Table III) and found to be smaller than the corresponding value measured at infinite dilution previously.<sup>10</sup> Combining this value with the ionization volume of water, which was found to be  $-19.9 \text{ cm}^3 \text{ mol}^{-1}$  at 1 M ionic strength compared to  $-22.1 \text{ cm}^3 \text{ mol}^{-1}$  at infinite dilution,<sup>13</sup> results in the reaction volume

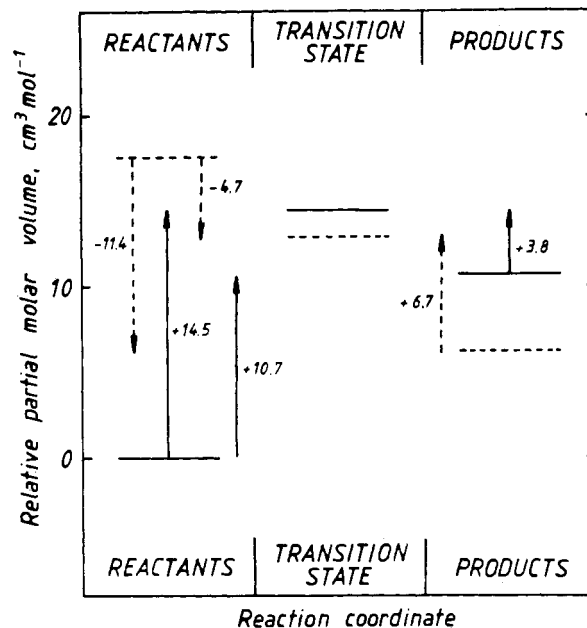


**Figure 1.** Volume profiles for reactions 1 and 2 at infinite dilution and 25 °C: reaction 1, solid lines; reaction 2, dashed lines.

for reaction 2. The values for  $\Delta V^\ddagger(k_2)$  and  $\Delta V^\ddagger(k_3)$  were subsequently estimated from the general expression given in (15).

$$\Delta \bar{V} = \Delta V^\ddagger(\text{forward reaction}) - \Delta V^\ddagger(\text{reverse reaction}) \quad (15)$$

According to the results in Table III, the volume data for reactions 1 and 2 exhibit very similar trends at zero and 1 M ionic strength. This means that the mechanistic interpretation will be very similar, and therefore the corresponding volume profiles are only presented for the data at zero ionic strength in Figure 1. A relative volume scale was adopted in the latter on the basis of the sum of the partial molar volumes of the reactants in reaction 1 set equal to zero. Quite surprising is the observation that the partial molar volume of the transition state in reaction 2 is very similar to that of reaction 1 (only  $1.6 \text{ cm}^3 \text{ mol}^{-1}$  smaller), notwithstanding the fact that the attacking species differ significantly, viz.  $\text{H}_2\text{O}$  as compared to  $\text{OH}^-$ . This similarity indicates that the geometries of the transition states for the coordination of  $\text{H}_2\text{O}$  and  $\text{OH}^-$  to the hfac ligand must be very similar in both cases. The value of  $\Delta V^\ddagger(k_3)$  is within the range of values usually found for the associative binding of a water molecule to various transition-metal complexes<sup>18</sup> and represents the bond formation component. The large difference between  $\Delta V^\ddagger(k_1)$  and  $\Delta V^\ddagger(k_3)$  can be ascribed to the overruling decrease in electrostriction due to charge neutralization when  $\text{OH}^-$  binds to  $\text{Co}(\text{en})_2(\text{hfac})^{2+}$  in reaction 1. Very large and positive  $\Delta V^\ddagger$  values were also found for closely related hydrolysis reactions involving the attack by  $\text{OH}^-$ .<sup>5,6</sup> Furthermore, the significance of the overall effect is also demonstrated by the significantly positive reaction volume for reaction 1. The value of  $\Delta V^\ddagger(k_2)$  can be interpreted in terms of an increase in volume due to bond cleavage accompanied by some volume decrease due to an increase in electrostriction. The larger volume of activation for the reverse step in reaction 2 indicates that bond cleavage is presumably not accompanied by an increase in electrostriction since the dissociation of  $\text{OH}^-$  involves a protonation preequilibrium followed by the release of  $\text{H}_2\text{O}$ .

The important role played by electrostriction in the forward step of reaction 1 also accounts for the particularly large ionic strength dependence of  $\Delta V^\ddagger(k_1)$ . Significantly smaller effects are observed for the remaining  $\Delta V^\ddagger$  values.

**Acknowledgment.** We gratefully acknowledge financial support from the Deutsche Forschungsgemeinschaft and the Fonds der Chemischen Industrie.

**Registry No.**  $\text{Co}(\text{en})_2(\text{hfac})^{2+}$ , 69496-09-9.

(16) Hamann, S. D. *J. Chem. Soc., Faraday Trans. 1* **1984**, *80*, 2541.

(17) The value for  $(\rho/\epsilon^3)^{1/2}$  in ref 14 was fitted to a quadratic equation.

(18) Reference 4, Chapters 3 and 4.